RESEARCH REPORTS
Biological

M.D. McKee[1]*, M.C. Yadav[2], B.L. Foster[3], M.J. Somerman[3], C. Farquharson[4], and J.L. Millán[2]

[1]Faculty of Dentistry, and Department of Anatomy and Cell Biology, Faculty of Medicine, McGill University, 3640 University Street, Montreal, QC, Canada; [2]Sanford Children's Health Research Center, Sanford-Burnham Medical Research Institute, La Jolla, CA, USA; [3]Laboratory for Oral Connective Tissue Biology, National Institute of Arthritis and Musculoskeletal and Skin Diseases, National Institutes of Health, Bethesda, MD, USA; and [4]Bone Biology Group, The Roslin Institute and Royal (Dick) School of Veterinary Studies, University of Edinburgh, Edinburgh, UK; *corresponding author, marc.mckee@mcgill.ca

J Dent Res 92(8):721-727, 2013

Compounded PHOSPHO1/ALPL Deficiencies Reduce Dentin Mineralization

ABSTRACT

Phosphatases are involved in bone and tooth mineralization, but their mechanisms of action are not completely understood. Tissue-nonspecific alkaline phosphatase (TNAP, ALPL) regulates inhibitory extracellular pyrophosphate through its pyrophosphatase activity to control mineral propagation in the matrix; mice without TNAP lack acellular cementum, and have mineralization defects in dentin, enamel, and bone. PHOSPHO1 is a phosphatase found within membrane-bounded matrix vesicles in mineralized tissues, and double ablation of *Alpl* and *Phospho1* in mice leads to a complete absence of skeletal mineralization. Here, we describe mineralization abnormalities in the teeth of *Phospho1*$^{-/-}$ mice, and in compound knockout mice lacking *Phospho1* and one allele of *Alpl* (*Phospho1*$^{-/-}$;*Alpl*$^{+/-}$). In wild-type mice, PHOSPHO1 and TNAP co-localized to odontoblasts at early stages of dentinogenesis, coincident with the early mineralization of mantle dentin. In *Phospho1* knockout mice, radiography, micro-computed tomography, histology, and transmission electron microscopy all demonstrated mineralization abnormalities of incisor dentin, with the most remarkable findings being reduced overall mineralization coincident with decreased matrix vesicle mineralization in the *Phospho1*$^{-/-}$ mice, and the almost complete absence of matrix vesicles in the *Phospho1*$^{-/-}$;*Alpl*$^{+/-}$ mice, whose incisors showed a further reduction in mineralization. Results from this study support prominent non-redundant roles for both PHOSPHO1 and TNAP in dentin mineralization.

KEY WORDS: matrix vesicles, tissue-non-specific alkaline phosphatase, extracellular matrix, extracellular matrix proteins, tooth, phosphatase.

DOI: 10.1177/0022034513490958

Received February 4, 2013; Last revision April 29, 2013; Accepted April 30, 2013

A supplemental appendix to this article is published electronically only at http://jdr.sagepub.com/supplemental.

INTRODUCTION

Mineralization in bones and teeth depends on systemic homeostasis of calcium and phosphate mineral ions, a suitable extracellular matrix protein scaffold, and the absence (and/or removal) of mineralization inhibitors (Murshed *et al*., 2004). Also involved, and particularly relevant to the early stages of tooth dentin and cartilage mineralization, are matrix vesicles (MVs). MVs are extracellular, nanometer-sized (~200 nm) membrane-invested bodies released from odontoblasts, osteoblasts, and chondroblasts/cytes that ultimately contain a precipitated carbonate-substituted hydroxyapatitic mineral phase (Anderson, 1969; Bernard, 1972; Eisenmann and Glick, 1972; Katchburian, 1973; Bonucci, 1984; Register *et al*., 1986). Following deposition of mineral within MVs, membrane rupture exposes the growing crystals to the extracellular matrix microenvironment, and other mineralization determinants are then thought to regulate the further growth of the crystals.

Phosphatases are clearly implicated in the mineralization process of bones and teeth, but their identities and functions remain unclear. Among these phosphatases, tissue-nonspecific alkaline phosphatase (TNAP, ALPL) is the best-characterized enzyme (Millan, 2006), promoting mineralization by restricting concentrations of mineralization-inhibiting pyrophosphate (PP_i) (Majeska and Wuthier, 1975; Meyer, 1984; Johnson *et al*., 2000; Hessle *et al*., 2002; Murshed *et al*., 2005). The loss of TNAP pyrophosphatase function results in the accumulation of PP_i in skeletal and dental tissues, leading to hypophosphatasia (HPP), characterized by rickets, osteomalacia, and, in odontohypophosphatasia, the premature loss of fully rooted teeth (Whyte, 2001). Mice lacking the TNAP gene (*Alpl*$^{-/-}$) phenocopy the infantile form of HPP (Narisawa *et al*., 1997; Fedde *et al*., 1999). In *Alpl*$^{-/-}$ mice, a mineralized skeleton is present at birth, but by post-natal days 6 to 10 there is generalized hypomineralization of the skeleton, with death by day 20. This is proposed to occur because of a block in the propagation of mineralization beyond the sheltered confines of the MV, attributable to accumulated levels of PP_i in the extracellular matrix resulting from lack of TNAP pyrophosphatase function (Anderson *et al*., 1997, 2004; Hessle *et al*., 2002; Millan, 2006). Indeed, MVs in both HPP patients and in *Alpl*$^{-/-}$ mice contain mineral crystals and thus retain the ability to initiate intravesicular mineralization in the absence of TNAP function (Anderson *et al*., 1997, 2004). These findings demonstrate that TNAP is not essential for the early stage of MV-mediated mineralization and suggest that other phosphatases may be involved.

Recent studies have implicated the enzyme PHOSPHO1 (phosphatase orphan 1, phosphoethanolamine/phosphocholine phosphatase) as being an important contributor to skeletal mineralization. PHOSPHO1 is an intravesicular phosphatase releasing phosphate from membrane-associated phosphoethanolamine and phosphocholine as part of an initial step in the process of MV-mediated mineralization (Roberts *et al*., 2004, 2007; Macrae *et al.*, 2010). Definitive evidence of a role for PHOSPHO1 in skeletal mineralization was confirmed by comparison of the bone phenotypes of *Phospho1*$^{-/-}$*;Alpl*$^{-/-}$ and *Phospho1*$^{-/-}$*;Alpl*$^{+/-}$ mice (Yadav *et al*., 2011). Whereas the *Alpl*$^{-/-}$ and *Phospho1*$^{-/-}$ individual knockout mice display hypomineralization of the skeleton, the double ablation of PHOSPHO1 and TNAP leads to a complete absence of skeletal mineralization and embryonic lethality, indicating independent, non-redundant mechanisms of action for both phosphatases in mineralization.

Of note from previous studies (Yadav *et al*., 2011) was the observation that *Phospho1*$^{-/-}$ mice were small. Metabolic studies suggested that reduced food and water consumption could be a contributing factor, and there was less visual evidence of food-pellet chewing in the mice lacking PHOSPHO1, consistent with the possibility of hypomineralized teeth and jaws. These observations, along with fundamental observations made previously on skeletal MV function in these mice and on the known importance of MVs in initiating mantle dentin mineralization (Bonucci, 1984; Ciancaglini *et al.*, 2010), led us to examine early stages of dentinogenesis in homozygous mice lacking PHOSPHO1 and in heterozygous mice lacking PHOSPHO1 and having only one allele of TNAP. Results from the present study support prominent roles for both PHOSPHO1 and TNAP in the mineralization of tooth dentin.

MATERIALS & METHODS

Mice

PHOSPHO1-R74X-null (*Phospho1*$^{-/-}$) mutant mice were generated by N-ethyl-N-nitrosourea (ENU) mutagenesis as previously described (Yadav *et al.*, 2011), as were the TNAP-null (*Alpl*$^{-/-}$) mice (Narisawa *et al*., 1997); mice were hybrids of C57Bl/6X129J mouse strains. *Phospho1*$^{-/-}$ mice were crossbred with *Alpl*$^{-/-}$ mice to generate compound *Phospho1*$^{-/-}$*;Alpl*$^{+/-}$ mice. Animal studies were conducted with approval from the Institutional Animal Care and Use Committee at Sanford-Burnham Medical Research Institute, accredited by AAALAC International (Multiple Project Assurance A3053-1).

Radiography

Radiographic images were taken under identical conditions for all mice by means of a Faxitron MX-20 (Faxitron X-ray Corporation, Wheeling, IL, USA). Digital images were recorded at 26 kV and 0.3 mA over a five-second exposure.

Micro-computed Tomography

Micro-computed tomography (Skyscan model 1072, Kontich, Belgium) of mandibles was performed for each genotype with an x-ray source operated at a power of 45 kv and at 222 μA, and x-ray sections covering a thickness of 124 μm in the longitudinal plane of the mesial root of the first and second molars, together with the underlying incisor and surrounding alveolar bone, were reconstructed with Skyscan tomography software (Skyscan).

Immunohistochemistry

Mandibles and maxillae from 18-day-old embryonic (E18) and four-day-old post-natal (P4) CD1 mice were immersion-fixed overnight in Bouin's solution, decalcified, and prepared for paraffin histology as previously described (Foster *et al*., 2013). Immunohistochemistry for PHOSPHO1 and TNAP on serial sections followed overnight incubation in 8.0 M guanidine HCl (pH 8.0). Primary antibodies were monoclonal human anti-PHOSPHO1 (recombinant Fab, AbD Serotec, MorphosysAG, Martinsried/Planegg, Germany) and monoclonal rat anti-human ALPL/TNAP (R&D Systems, Minneapolis, MN, USA), followed by biotinylated secondary antibodies (Vectastain Elite ABC, Vector Labs, Burlingame, CA, USA). Red color reactions were obtained with 3-amino-9-ethylcarbazole (AEC; substrate kit, Vector Labs).

Light and Electron Microscopy

Immersion-fixed (1% glutaraldehyde plus 4% paraformaldehyde, 0.1 M sodium cacodylate buffer, pH 7.3), ethanol-dehydrated, and Epon-embedded undecalcified mandibles from P10 mice were sectioned at the level of the first molar or second molar, together with the underlying incisor and surrounding alveolar bone. Thin sections (1 μm) were stained for mineral with 3% silver nitrate (von Kossa reagent); counterstaining was with toluidine blue. Frontal sections at the same level of the most mesial root of the first molar provided longitudinally sectioned molar and cross-sectioned incisor (with alveolar bone) image planes for comparative histological analyses. Ultrastructural observations were made by transmission electron microscopy (TEM; FEI Technai 12, Hillsboro, OR, USA). TEM energy-dispersive x-ray spectroscopy and selected-area electron diffraction were used for elemental analysis and mineral phase identification, respectively.

RESULTS

Coincident Expression of PHOSPHO1 and TNAP during Odontogenesis

Immunohistochemical staining for PHOSPHO1 and TNAP in serial sections provided comparative spatiotemporal mapping of these 2 proteins in normal developing mouse molars, incisors, and alveolar bone. In E18 mice, PHOSPHO1 (Fig. 1A) and TNAP (Fig. 1B) both localized to osteoblasts at forming bone surfaces, consistent with previous reports for other skeletal sites (Houston *et al*., 2004; Roberts *et al*., 2007). For teeth, at this early bell stage prior to mineralization, PHOSPHO1 was not detected in the molar, whereas TNAP was more widely expressed in osteoblasts as well as in some portions of the enamel organ. At the later P4 stage of development, PHOSPHO1 (Figs. 1C, 1E) and TNAP (Figs. 1D, 1F) again localized to osteoblasts and to odontoblasts, coinciding with differentiation of these cells and the appearance of the initial layer of mantle dentin

(Figs. 1E, 1F). While TNAP strongly stained the entire odontoblast layer of the developing molar, the strongest staining for PHOSPHO1 was in newly differentiated odontoblasts as compared with the weaker staining of older odontoblasts found more occlusally. PHOSPHO1 immunostaining was also found in ameloblasts throughout crown formation, whereas TNAP was expressed in ameloblasts only at certain stages of amelogenesis (Yadav *et al*., 2012). Localization patterns for PHOSPHO1 and TNAP in the incisor paralleled those of the molar, namely, showing consistent staining of odontoblasts in mineralizing regions (Figs. 1G, 1H). Additional PHOSPHO1 immunohistochemistry at different ages is shown in Appendix Fig. 1.

Reduced Dentin Mineralization in *Phospho1*$^{-/-}$ and *Phospho1*$^{-/-}$;*Alpl*$^{+/-}$ Mice

Radiography, histology, and micro-computed tomography of mandibles from P10 wild-type mice showed well-mineralized bones and teeth at the level of the first and second molars (Figs. 2A-2F). Similar analyses at these identical sites in *Phospho1*$^{-/-}$ mice (Figs. 2G-2L) showed reduced mineralization of alveolar bone (Fig. 2H) and incisor dentin (Fig. 2K, 2L). This reduction was even more pronounced with the deletion of one TNAP allele in the *Phospho1*$^{-/-}$ background (*i.e*., the *Phospho1*$^{-/-}$;*Alpl*$^{+/-}$ mice) (Figs. 2M-2R), in which osteoidosis in the bone was readily apparent (Fig. 2N) and the mineralization defect in the incisor (Fig. 2O-R) extended occlusally beyond the second molar and into the level of the first molar.

Quantitative micro-computed tomography mineralization data are given for incisors in Appendix Fig. 2, where highly statistically significant differences in mineralization were observed in all mice, with *Phospho1*$^{-/-}$;*Alpl*$^{+/-}$ mice showing the greatest reduction in incisor mineralization. Molar development and mineralization for both *Phospho1*$^{-/-}$ and *Phospho1*$^{-/-}$;*Alpl*$^{+/-}$ mice seemed largely unaffected.

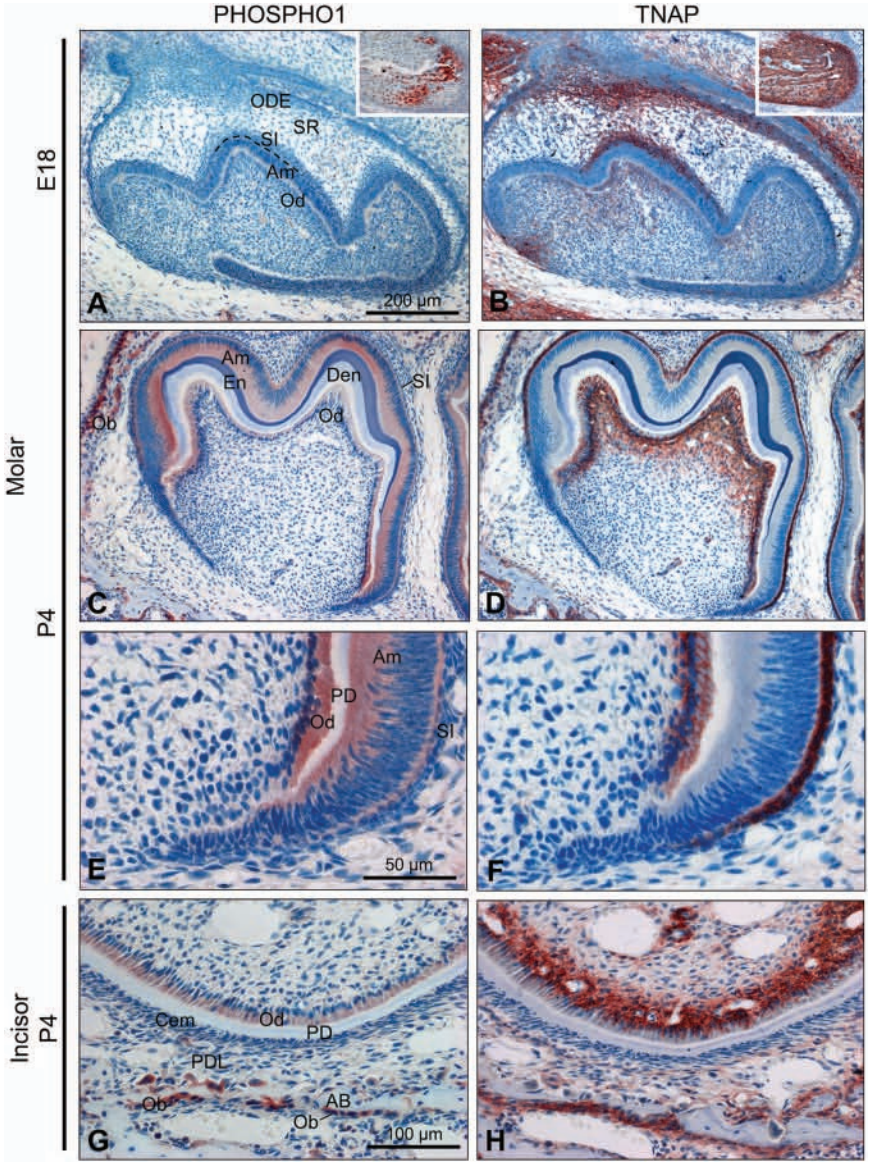

Figure 1. Coincident expression of PHOSPHO1 and TNAP during odontogenesis. Immunohistochemistry showing the spatiotemporal expression of PHOSPHO1 and TNAP in serial sections of developing mouse molars and incisors. **(A)** At the early bell stage at embryonic age E18, prior to mineralization, PHOSPHO1 is not detected in the molar, but strongly localizes to mandibular bone, especially on actively forming surfaces (inset). **(B)** At E18, TNAP is more widely localized to developing bone (inset) and some regions of the molar enamel organ, including the stellate reticulum, stratum intermedium, and outer dental epithelium. **(C-F)** At the later bell stage at post-natal age P4, both PHOSPHO1 and TNAP localize to alveolar bone osteoblasts, and co-localize to newly differentiating odontoblasts and the appearance of predentin matrix. PHOSPHO1 is also present in ameloblasts throughout crown formation. **(G, H)** In the mouse incisor, PHOSPHO1 and TNAP localization patterns parallel those seen in the molar, with both being found in odontoblasts associated with mineralizing dentin, and in osteoblasts lining the surrounding bone. TNAP localizes more widely in the incisor to sub-odontoblast pulp and periodontal ligament. Outer dental epithelium (ODE); stellate reticulum (SR); stratum intermedium (SI); ameloblasts (Am); odontoblasts (Od); enamel (En); dentin (Den); predentin (PD); cementoblasts (Cem); periodontal ligament (PDL); alveolar bone (AB); and osteoblasts (Ob).

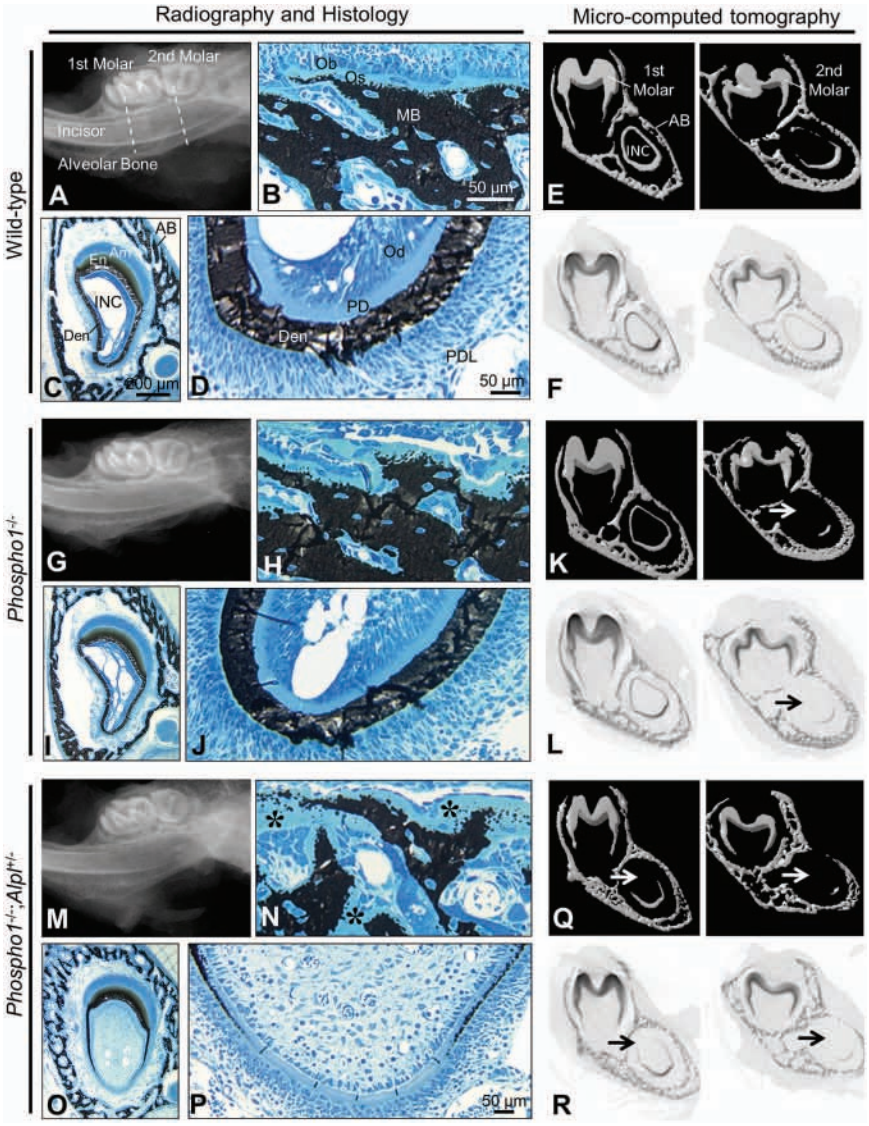

Figure 2. Dentin mineralization is reduced in *Phospho1*$^{-/-}$ and *Phospho1*$^{-/-}$*;Alpl*$^{+/-}$ mice. Radiography, histology (black von Kossa staining for mineral), and micro-computed tomography of 10-day-old mandibles. Dashed lines indicate cross-sectional planes observed by histology and micro-computed tomography at the level of the first and second molars. Compared with wild-type controls **(A-F)**, a reduction in mineralization of root analog dentin (arrow) is observed in the incisor of *Phospho1*$^{-/-}$ mice **(G-L)**, particularly at the level of the second molar. In *Phospho1*$^{-/-}$*;Alpl*$^{+/-}$ mice **(M-R)**, bone osteoidosis is apparent (asterisks), and incisor root analog dentin mineralization is reduced further, extending beyond the level of the second molar to the level of the first molar (arrows). All histology sections shown are of the incisor and the surrounding alveolar bone taken at the level of the first molar. [For quantification of incisor mineralization, see Appendix Fig. 1.] Osteoblasts (Ob); osteoid (Os); mineralized bone (MB); alveolar bone (AB); incisor (INC); ameloblasts (Am); enamel (En); dentin (Den); predentin (PD); odontoblasts (Od); and periodontal ligament (PDL).

Transmission Electron Microscopy of Abnormalities in Mantle Dentin Mineralization and Matrix Vesicles in *Phospho1*$^{-/-}$ and *Phospho1*$^{-/-}$*;Alpl*$^{+/-}$ Mice

TEM of normal mineralizing mantle dentin in P10 wild-type incisors revealed ultrastructural features consistent with those reported previously (shown here sequentially from less to more mineralized in Figs. 3A-3F). MVs produced by odontoblasts were abundant in mantle dentin (Figs. 3A, 3B), eventually mineralizing with small crystal deposits of hydroxyapatite and then rupturing, leading to small patches/foci of mineralized mantle dentin (Fig. 3C). These foci enlarge and coalesce to extend as a wide mineralized tract throughout the extracellular matrix of the dentin (Figs. 3D-3F).

In the mantle dentin of P10 *Phospho1*$^{-/-}$ incisors showing reduced mineralization by micro-computed tomography, TEM revealed seemingly normal dentin ultrastructure with an abundance of MVs and both small foci of mineralization and larger patches of mineralized matrix (Figs. 4A-4D). MVs appeared to be more abundant than in normal mantle dentin, but were less frequently mineralized and with less mineral.

In the mantle dentin of P10 *Phospho1*$^{-/-}$*; Alpl*$^{+/-}$ incisors showing an even greater reduction in dentin mineralization attributable in these mice to the additional removal of one allele of TNAP, we noted by TEM an almost complete loss of MVs in the mantle dentin (Figs. 4E-4H). While MVs were generally absent, there was nevertheless some degree of mineralization occurring within the matrix, appearing initially as small diffuse patches among the mantle dentin collagen fibrils (Figs. 4F, 4G). These were distinctly different from the more sharply bordered foci/patches observed in the other genotypes; nonetheless, they contained apatitic mineral, as determined by x-ray microanalysis (Fig. 4F inset) and electron diffraction (Fig. 4G inset). As mineralization progressed in the mantle dentin and the mineralized matrix patches became larger, while reduced, they became similar to those observed at earlier stages in the other genotypes.

DISCUSSION

Previously we have shown that PHOSPHO1 and TNAP expression overlap during chick skeletal development (Macrae *et al*., 2010) and that double ablation of TNAP and PHOSPHO1 functions leads to a complete absence of skeletal mineralization and embryonic lethality in the mouse (Yadav *et al*., 2011). We also confirmed that PHOSPHO1 and TNAP have prominent functions in establishing an appropriate P_i/PP_i ratio conducive to proper matrix

mineralization in bone (Millán, 2013). Consistent with these findings, we show here the coordinated and overlapping expression of TNAP and PHOSPHO1 during odontogenesis, and report on tooth dentin abnormalities in PHOSPHO1-knockout mice that worsen when one allele of TNAP is additionally ablated. Since double-null *Phospho1*$^{-/-}$;*Alpl*$^{-/-}$ mice are embryonic-lethal, we analyzed postnatal tooth development in compound knockout mice lacking only one allele for TNAP.

While the reduction in mineralization of dentin in both *Phospho1*-null and *Phospho1*$^{-/-}$;*Alpl*$^{+/-}$ mice is particularly noteworthy, the most remarkable finding in our view is the nearly complete absence of MVs in the mantle dentin of the *Phospho1*$^{-/-}$;*Alpl*$^{+/-}$ mice. These findings are in agreement with recent preliminary data reporting reduced MVs associated with reduced expression of PHOSPHO1 and TNAP in odontoblasts when the *Trps1* gene is down-regulated with shRNA (Kuzynski *et al*., 2013). However, the apparent lack of MVs in the mantle dentin from *Phospho1*$^{-/-}$;*Alpl*$^{+/-}$ mice is in contrast to the apparent increased numbers of MVs devoid of mineral observed in metatarsal bone of a single *Phospho1*$^{-/-}$;*Alpl*$^{-/-}$ stillborn pup (Yadav *et al*., 2011), pointing to a potential differential response of odontoblasts and chondroblasts/osteoblasts to changes in the P_i/PP_i ratio. It is recognized that unambiguous identification and characterization of membrane-bound vesicular structures in dentin are especially difficult, for several reasons. First, cross-sections of fine odontoblast processes are about the same size as matrix vesicles and look similar by transmission electron microscopy. Second, re-annealing of membranes may occur during biochemical isolation procedures which could reduce and/or increase the number of vesicles. Third, there are no discriminating MV markers readily detectable by ultrastructure analyses. Despite this, analysis of the present data provides clear evidence for a dentin mineralization defect linked to a loss of mantle dentin MVs in mice lacking (or having reduced) key enzymes involved in P_i and PP_i processing essential to bone and tooth mineralization. Indeed, the contribution of MVs to mineralization of vertebrate extracellular matrices is widely thought to be best exemplified by that seen prominently in tooth mantle dentin. Analysis of our data showing that the loss of MVs associates with reduced dentin mineralization confirms this important role for MVs in teeth, and underscores the importance of the 2 enzymes studied here (PHOSPHO1 and TNAP) to contribute to this mineralization process. Perhaps most importantly, these data point to the possibility that changes in MV biogenesis (and in turn affecting mineralization) may occur as a result of an altered extracellular P_i/PP_i ratio in skeletal and dental tissues regulated at least in part by these 2 enzymes. While clearly implicated by the present study in incisor dentin mineralization, it is less clear why changes in the levels of these 2 phosphatases

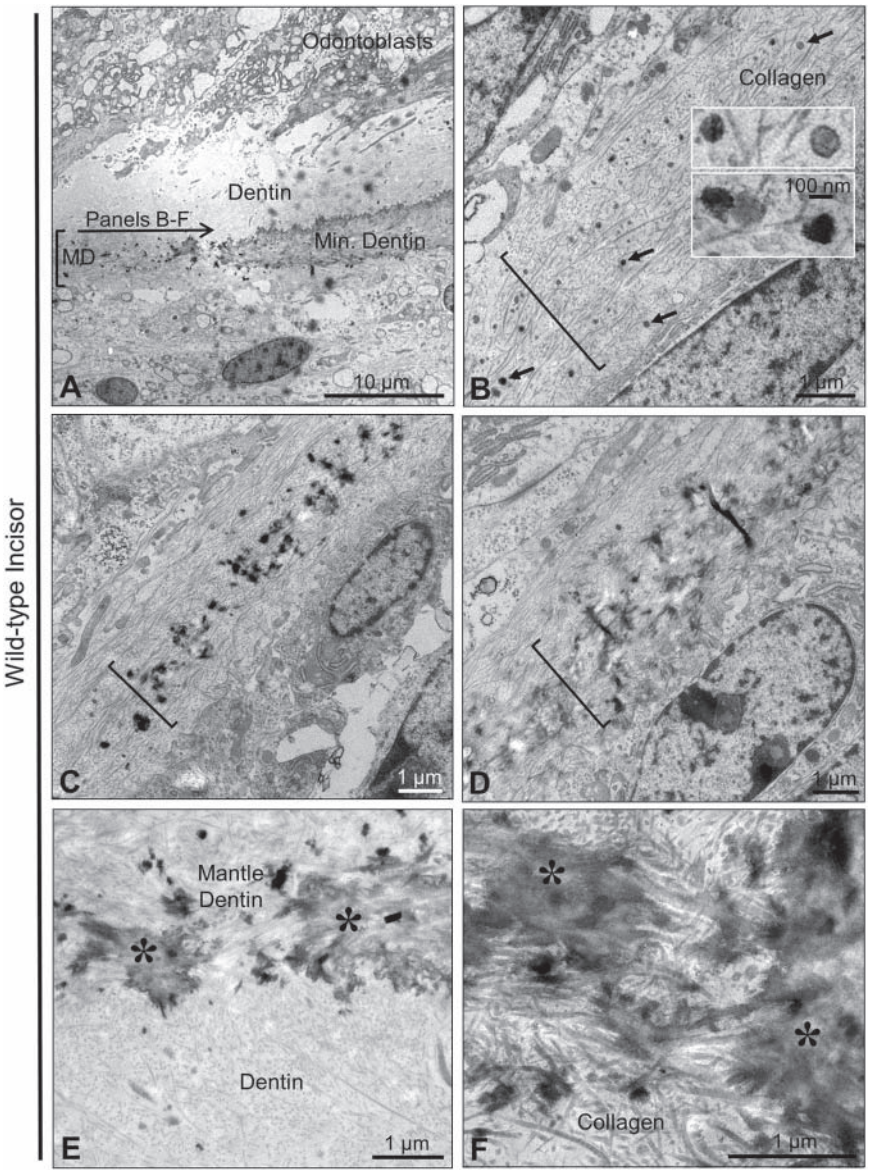

Figure 3. Transmission electron microscopy of mantle dentin mineralization and matrix vesicles in control wild-type mouse incisor. **(A-F)** Sequential electron micrographs of 10-day-old incisor dentin proceeding from less to more mineralized matrix regions. Matrix vesicles (arrows, insets) and mineralization (asterisks) first appear as isolated structures among the collagen fibrils in the mantle dentin (MD, brackets), with mineralization proceeding initially within matrix vesicles, and then progressing as a propagation/enlargement of small mineralization foci to form large, coalesced regions of mineralized matrix.

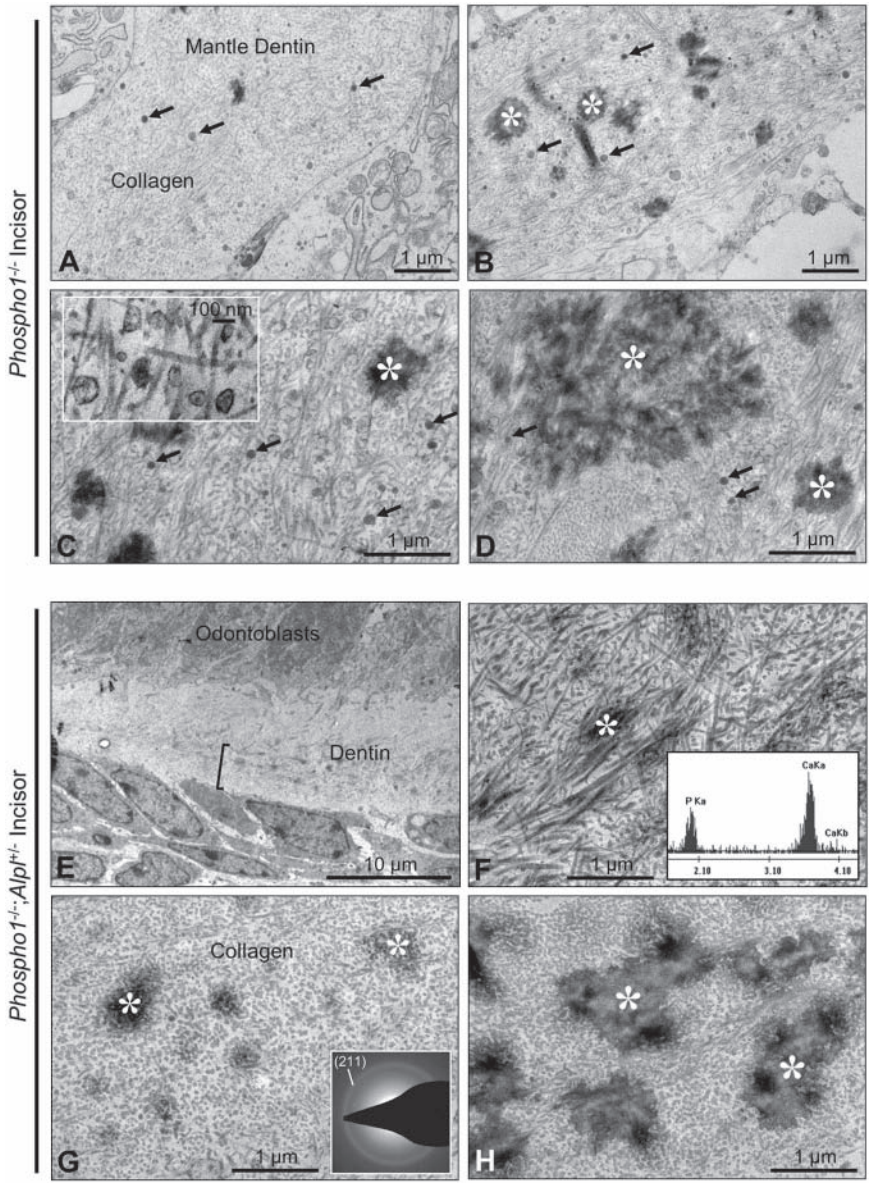

Figure 4. Transmission electron microscopy of abnormal mantle dentin mineralization and matrix vesicles in *Phospho1*$^{-/-}$ and *Phospho1*$^{-/-}$*;Alpl*$^{+/-}$ mice. Sequential electron micrographs of 10-day-old incisor dentin proceeding from less to more mineralized matrix regions in *Phospho1*$^{-/-}$ **(A-D)** and *Phospho1*$^{-/-}$*;Alpl*$^{+/-}$ **(E-H)** mice. Abundant matrix vesicles (arrows, and panel C inset) and small mineralization foci (asterisks) are present in the mantle dentin among the collagen fibrils of *Phospho1*$^{-/-}$ mice, but matrix vesicle mineralization appears to be reduced. In *Phospho1*$^{-/-}$*;Alpl*$^{+/-}$ mice, matrix vesicles are generally absent from the mantle dentin (bracket), yet small mineralization foci can be observed (asterisks) that enlarge over time as mineralization progresses. X-ray microanalysis (inset in panel F) and electron diffraction (inset in panel G) confirm the presence of calcium and phosphorus at mineralization foci, and that the mineral phase is apatitic (having major 211 diffraction maxima), respectively.

do not equally affect molar crown dentin mineralization. Differences in their expression levels, together with differences in dentin matrix composition, may account for this unexplained finding—and several published reports have documented differences in crown *vs*. root dentin biology (Beertsen and Niehof, 1986; Takagi *et al.*, 1988; Kaipatur *et al*., 2008)—as might undetermined downstream effects of continuous eruption in the incisors of rodents which maintain a different stem cell niche. It is not yet clear whether cementum is affected in the knockout mice and whether MVs are involved in its mineralization.

Integrating these findings, our unified model starts with the MVs as a site of initiation of mineralization. Hydroxyapatite crystals appear inside MVs favored by Pi accumulation resulting from a dual mechanism involving PHOSPHO1-mediated intravesicular production of Pi together with transporter-mediated influx of Pi produced extravesicularly primarily by TNAP's ATPase activity or by NPP1's ATPase activity. Organophosphate compounds (ATP) and perhaps also PPi are the source of Pi for this initial step of mineralization. Subsequent extravesicular mineralization is promoted primarily by TNAP's pyrophosphatase activity, and secondarily by NPP1's pyrophosphatase activity, and is driven by the availability of Pi and the presence of a collagenous fibrillar scaffold while being guided by other matrix mineral-binding proteins (Yadav *et al*., 2011; Millán, 2013).

ACKNOWLEDGMENTS

This work was funded by the CIHR (MOP97858-MDM), the NIH (DE12889 and AR53102-JLM), an Institute Strategic Program Grant from the Biotechnology and Biological Sciences Research Council, UK (CF), and the Intramural Program of NIAMS/NIH (MJS). MDM is a member of the FRQ-S Network in Oral and Bone Health Research. The authors thank Lydia Malynowsky and Valentin Nelea for assistance with microscopy, and Laura Zweifler for assistance with antibody screening. The authors declare no potential conflicts of interest with respect to the authorship and/publication of this article.

REFERENCES

Anderson H, Sipe J, Hessle L, Dhanyamraju R, Atti E, Camacho N, *et al*. (2004). Impaired calcification around matrix vesicles of growth plate and bone in alkaline phosphatase-deficient mice. *Am J Pathol* 164:841-847.

Anderson HC (1969). Vesicles associated with calcification in the matrix of epiphyseal cartilage. *J Cell Biol* 41:59-72.

Anderson HC, Hsu HH, Morris DC, Fedde KN, Whyte MP (1997). Matrix vesicles in osteomalacic hypophosphatasia bone contain apatite-like mineral crystals. *Am J Pathol* 151:1555-1561.

Beertsen W, Niehof A (1986). Root-analogue versus crown-analogue dentin: a radioautographic and ultrastructural investigation of the mouse incisor. *Anat Rec* 215:106-118.

Bernard GW (1972). Ultrastructural observations of initial calcification in dentine and enamel. *J Ultrastruct Res* 41:1-17.

Bonucci E (1984). Matrix vesicles: their role in calcification. In: Dentin , dentinogenesis Linde. A, editor. Boca Raton, FL: CRC Press, pp. 135-154.

Ciancaglini P, Yadav MC, Simão AM, Narisawa S, Pizauro JM, Farquharson C, *et al*. (2010). Kinetic analysis of substrate utilization by native and TNAP-, NPP1-, or PHOSPHO1-deficient matrix vesicles. *J Bone Miner Res* 25:716-723.

Eisenmann DR, Glick PL (1972). Ultrastructure of initial crystal formation in dentin. *J Ultrastruct Res* 41:18-28.

Fedde K, Blair L, Silverstein J, Coburn S, Ryan L, Weinstein R, *et al*. (1999). Alkaline phosphatase knock-out mice recapitulate the metabolic and skeletal defects of infantile hypophosphatasia. *J Bone Miner Res* 14:2015-2026.

Foster BL, Nagatomo KJ, Tso HW, Tran AB, Nociti FH, Narisawa S, *et al*. (2013). Tooth root dentin mineralization defects in a mouse model of hypophosphatasia. *J Bone Miner Res* 28:271-282.

Hessle L, Johnson K, Anderson H, Narisawa S, Sali A, Goding J, *et al*. (2002). Tissue-nonspecific alkaline phosphatase and plasma cell membrane glycoprotein-1 are central antagonistic regulators of bone mineralization. *Proc Natl Acad Sci USA* 99:9445-9449.

Houston B, Stewart AJ, Farquharson C (2004). PHOSPHO1-A novel phosphatase specifically expressed at sites of mineralisation in bone and cartilage. *Bone* 34:629-637.

Johnson K, Hessle L, Vaingankar S, Wennberg C, Mauro S, Narisawa S, *et al*. (2000). Osteoblast tissue-nonspecific alkaline phosphatase antagonizes and regulates PC-1. *Am J Physiol Regul Integr Comp Physiol* 279:R1365-1377.

Kaipatur NR, Murshed M, McKee MD (2008). Matrix Gla protein inhibition of tooth mineralization. *J Dent Res* 87:839-844.

Katchburian E (1973). Membrane-bound bodies as initiators of mineralization of dentine. *J Anat* 116(Pt 2):285-302.

Kuzynski M, Mobley C, Yadav M, Winters T, Butler A, Kellermann O, *et al*. (2013). Trps1 is required for mineralization of odontoblastic cells in vitro. *J Dent Res* 92(Spec Iss B):Abstract #2032. IADR General Session, Seattle WA. Accessed on 4/30/2013 at: http://iadr.confex.com/iadr/13iags/webprogram/Paper174990.html.

Macrae VE, Davey MG, McTeir L, Narisawa S, Yadav MC, Millan JL, *et al*. (2010). Inhibition of PHOSPHO1 activity results in impaired skeletal mineralization during limb development of the chick. *Bone* 46:1146-1155.

Majeska RJ, Wuthier RE (1975). Studies on matrix vesicles isolated from chick epiphyseal cartilage. Association of pyrophosphatase and ATPase activities with alkaline phosphatase. *Biochim Biophys Acta* 391:51-60.

Meyer JL (1984). Can biological calcification occur in the presence of pyrophosphate? *Arch Biochem Biophys* 231:1-8.

Millan JL (2006). Mammalian alkaline phosphatases: from biology to applications in medicine and biotechnology. Weinheim, Germany: Wiley-VCH, pp. 1-322.

Millán JL (2013). The role of phosphatases in the initiation of skeletal mineralization. *Calcif Tissue Int* [Epub ahead of print 11/27/2012] (in press).

Murshed M, Schinke T, McKee MD, Karsenty G (2004). Extracellular matrix mineralization is regulated locally; different roles of two gla-containing proteins. *J Cell Biol* 165:625-630.

Murshed M, Harmey D, Millán J, McKee M, Karsenty G (2005). Unique coexpression in osteoblasts of broadly expressed genes accounts for the spatial restriction of ECM mineralization to bone. *Genes Dev* 19:1093-1104.

Narisawa S, Fröhlander N, Millán J (1997). Inactivation of two mouse alkaline phosphatase genes and establishment of a model of infantile hypophosphatasia. *Dev Dyn* 208:432-446.

Register TC, McLean FM, Low MG, Wuthier RE (1986). Roles of alkaline phosphatase and labile internal mineral in matrix vesicle-mediated calcification. Effect of selective release of membrane-bound alkaline phosphatase and treatment with isosmotic pH 6 buffer. *J Biol Chem* 261:9354-9360.

Roberts S, Narisawa S, Harmey D, Millán J, Farquharson C (2007). Functional involvement of PHOSPHO1 in matrix vesicle-mediated skeletal mineralization. *J Bone Miner Res* 22:617-627.

Roberts SJ, Stewart AJ, Sadler PJ, Farquharson C (2004). Human PHOSPHO1 exhibits high specific phosphoethanolamine and phosphocholine phosphatase activities. *Biochem J* 382(Pt 1):59-65.

Takagi Y, Nagai H, Sasaki S (1988). Difference in noncollagenous matrix composition between crown and root dentin of bovine incisor. *Calcif Tissue Int* 42:97-103.

Whyte MP (2001). Hypophosphatasia. In: The metabolic and molecular bases of inherited disease. Scriver C, Beaudet A, Sly W, Valle D, Childs B, Kinzler K, editors. New York, NY: McGraw-Hill, pp. 5313-5329.

Yadav MC, Simão AM, Narisawa S, Huesa C, McKee MD, Farquharson C, *et al*. (2011). Loss of skeletal mineralization by the simultaneous ablation of PHOSPHO1 and alkaline phosphatase function: a unified model of the mechanisms of initiation of skeletal calcification. *J Bone Miner Res* 26:286-297.

Yadav MC, de Oliveira RC, Foster BL, Fong H, Cory E, Narisawa S, *et al*. (2012). Enzyme replacement prevents enamel defects in hypophosphatasia mice. *J Bone Miner Res* 27:1722-1734.